

# Diels–Alder Trapping of Photochemically Generated *o*-Quinodimethane Intermediates: An Alternative Route to Photocured Polymer Film Development

Daniel S. Tyson,<sup>†,§</sup> Faysal Ilhan,<sup>†,§</sup> Mary Ann B. Meador,<sup>§</sup> Dee Dee Smith,<sup>‡,§</sup> Daniel A. Scheiman,<sup>‡</sup> and Michael A. Meador<sup>\*,§</sup>

Ohio Aerospace Institute, 22800 Cedar Point Road, Cleveland, Ohio 44142, NASA Glenn Research Center, 21000 Brookpark Road, Cleveland, Ohio 44135, and QSS Group, Inc., 4500 Forbes Boulevard Suite 200, Lanham, Maryland 20706

Received August 19, 2004; Revised Manuscript Received February 8, 2005

**ABSTRACT:** Photolysis of *o*-methylphenyl ketones generates *o*-quinodimethane intermediates that can be trapped in situ by dienophiles through Diels–Alder cycloadditions. This well-known photochemical process is applied to a series of six new photoreactive monomers containing bis(*o*-methylphenyl ketone) functionalities combined with diacrylate and triacrylate esters for the development of acrylic ester copolymer blends. Irradiation of cyclohexanone solutions of the bis(*o*-methylphenyl ketone)s and acrylate esters produce thin polymer films. Solid state <sup>13</sup>C NMR data indicated 47–100% reaction of the bis(*o*-methylphenyl ketone)s, depending on experimental conditions, to yield the desired products. DSC and TGA analyses were performed to determine the glass transition temperature, *T*<sub>g</sub>, and onset of decomposition, *T*<sub>d</sub>, of the resulting polymer films. A statistical “design of experiments” approach was used to obtain a systematic understanding of the effects of experimental variables on the extent of polymerization and the final polymer properties.

## Introduction

Diels–Alder cycloadditions have often been utilized in polymer synthesis as an alternative to condensation reactions.<sup>1</sup> These methods are attractive for use in the preparation of high performance polymers, such as polyimides, because they utilize monomers that have less environmental, health, and safety risks. In addition, they have the potential to be adapted to low cost processing techniques, including resin transfer molding.

Typical Diels–Alder cycloadditions employ bis(dienes), such as bis(furans), and bis(dienophiles), such as bis(maleimides) or bis(acrylates). An alternative approach that has received some attention involves Diels–Alder cycloadditions with thermolytically generated reactive bis(diene) intermediates. One example of this utilizes *o*-quinodimethanes which are produced by the thermolysis of benzocyclobutane precursors.<sup>2</sup> While this approach provides polymers with high glass transition temperatures and good thermal stabilities; it typically requires reaction temperatures in excess of 200 °C and reaction times on the order of 1–8 h. Future NASA Human and Robotic Exploration missions will require polymers and adhesives that may be cured in ambient space environments for in-space repairs, large deployable, rigidizable arrays and inflatable habitats and rovers. On Earth, lower cure temperatures are desirable to reduce tooling costs and processing induced thermal stresses, which can lead to microcracking and delaminations especially in fiber reinforced composites. In addition, thermal processing conditions may be too severe to use with certain functional groups, such as

nonlinear optically active or antimicrobial units. For these reasons, we have been pursuing the development of high performance polymers that can be cured at low temperatures with ultraviolet radiation, rather than heat.

Along these lines, we have previously reported a method for the preparation of linear aromatic polyimides by exploiting Diels–Alder cycloaddition reactions of bis-*o*-quinodimethanes<sup>3</sup>, which are generated in situ by a classical photochemical reaction: the photoenolization of *o*-methylphenyl ketones.<sup>4</sup> As depicted in Scheme 1, photolysis of *o*-methylbenzophenone (**1**) produces a pair of hydroxy-*o*-quinodimethane isomers (**3Z** and **3E**) via a 1,4-biradical intermediate (**2**). The quinodimethane isomer, **3Z**, is unstable and reverts to the starting material with high efficiency. However, **3E** can be trapped by Diels–Alder cycloaddition with dienophiles, including dimethyl acetylenedicarboxylate (**3d**), to produce the corresponding cycloadducts.<sup>5</sup> Polyimides prepared from this chemistry in dilute benzene or cyclohexanone solutions have glass transition temperatures above 300 °C and good thermal-oxidative stability (*T*<sub>d</sub>'s in air in excess of 330 °C). Later attempts to prepare polyimide films from more concentrated cyclohexanone solutions produced films which adhere well to various substrates (glass, aluminum) but are brittle.

A variety of chemical structures, such as ether linkages and molecular twists, are known to improve the processability and ductility of high performance polymers.<sup>6</sup> In an attempt to produce polymer films with greater ductility and flexibility, a series of six new bis(*o*-methylphenyl ketone) monomers were prepared containing these units (Table 1, **5–10**). These new diketone monomers were irradiated in the presence of diacrylates and triacrylates to produce polymer blends via Diels–Alder cycloadditions of the photoenols. The results of these experiments are presented herein.

\* Corresponding author. E-mail: Michael.A.Meador@grc.nasa.gov.

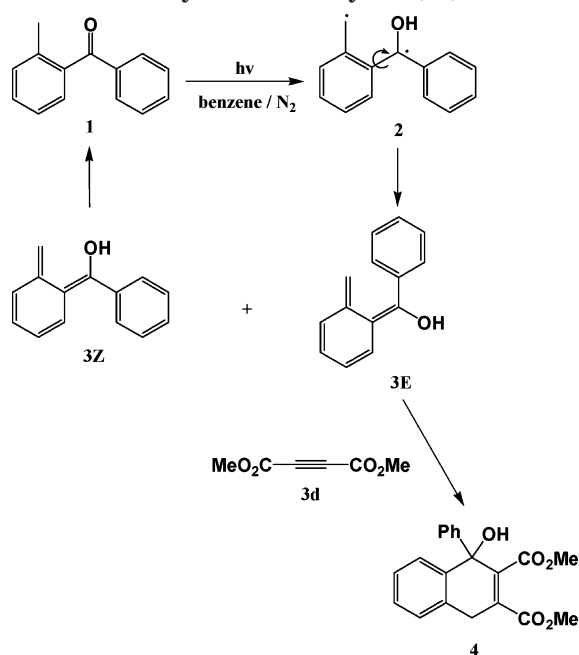
<sup>†</sup> Ohio Aerospace Institute.

<sup>‡</sup> NASA Undergraduate Researcher's Program, 2002 and 2003. Currently at Northwestern University.

<sup>§</sup> NASA Glenn Research Center.

<sup>‡</sup> QSS Group, Inc.

**Scheme 1. Photoenolization of *o*-Methylbenzophenone (1) and Subsequent Diels–Alder Trapping with Dimethyl Acetylenedicarboxylate (3d)**



## Experimental Section

**Materials.** 1,6-Hexanediol ethoxylate diacrylate (11), pentaerythritol triacrylate (12), and methyl acrylate (13) were purchased from the Aldrich Chemical Co. and stored in the dark at less than 10 °C. Tetrahydrofuran (THF) was obtained from Aldrich and purified by distillation using potassium/benzophenone as drying agents. Triethylene glycol monomethyl ether tosylate (PEG–TOS) was prepared according to a literature procedure.<sup>7</sup> All other reagents were purchased from commercial sources and used without further purification.

**General Synthesis of Dinitriles (A).** Phenol or bisphenol (1 equiv, ca. 1 mol) was dissolved in dimethyl sulfoxide (DMSO) (100 mL) in a 500 mL, three-neck round-bottom flask equipped with a Dean–Stark trap, a condenser, and nitrogen inlet. Anhydrous  $K_2CO_3$  (1 equiv, ca. 1 mol) and 100 mL of benzene were added. The mixture was heated (90 °C) with stirring for 18 h or until the level of collected water became constant. The remaining benzene was removed by distillation and the reaction mixture was allowed to cool to room temperature. 4-Nitrobenzonitrile (1 or 2 equiv, ca. 1 or 2 mol) was added directly to the reaction flask. The reaction was stirred at 100 °C for 72 h, and then allowed to cool to room temperature. The resulting mixture was poured into a flask containing 1 L of distilled water. The flask was cooled in an ice bath and the product was allowed to precipitate overnight. The crude product was then filtered and dried under vacuum. The resulting solid was recrystallized from hot ethanol and dried under vacuum.

**4,4'-Dicyanodiphenyl Ether (7a).** 50% yield (mp 179–181 °C).  $^1H$  (200 MHz,  $CDCl_3$ ):  $\delta$  6.94 (d,  $J$  = 8 Hz, 2H), 7.50 (d,  $J$  = 8 Hz, 2H).

**2,2'-Bis(4-(2-methylbenzoyl)phenoxy)biphenyl (8a).** 33% yield (mp 145–147 °C).  $^1H$  (200 MHz,  $CDCl_3$ ):  $\delta$  6.62 (d,  $J$  = 8 Hz, 4H), 6.81 (d,  $J$  = 8 Hz, 2H), 7.02–7.19 (m, 6H), 7.28 (d,  $J$  = 8 Hz, 4H).

**2,2-Bis(2-(4-cyanophenoxy)phenyl) propane (9a).** 79% yield (mp 122–124 °C).  $^1H$  (200 MHz,  $CDCl_3$ ):  $\delta$  1.68 (s, 6H), 6.85 (m, 8H), 7.09 (d,  $J$  = 8 Hz, 4H), 7.40 (d,  $J$  = 8 Hz, 4H).

**2,2-Bis(2(4-cyanophenoxy)phenyl)-1,1,1,3,3,3-hexafluoropropane (10a).** 90% yield (mp 161–163 °C).  $^1H$  (200 MHz,

$CDCl_3$ ):  $\delta$  7.04 (m, 8H), 7.38 (d,  $J$  = 8 Hz, 4H), 7.59 (d,  $J$  = 8 Hz, 4H).

**General Synthesis of Diketones (B).** To a stirred solution of the corresponding dinitrile in dry THF under nitrogen was added dropwise a THF solution of either 4-methoxy phenylmagnesium bromide (reaction B<sub>1</sub>) or 2-methyl phenylmagnesium bromide (reaction B<sub>2</sub>). The resulting mixture was refluxed under nitrogen for 18 h. The reaction mixture was then allowed to cool to room temperature and poured into a saturated aqueous  $NH_4Cl$  solution. The organic phase was collected and the aqueous phase extracted with THF. The organic extracts were combined and dried over  $Na_2SO_4$ . The solvent was dried in vacuo to yield the crude product. A (1:1) mixture of concentrated HCl and water was added to that product and the resulting mixture was refluxed for 18 h. The mixture was then cooled to room temperature and extracted with  $CH_2Cl_2$ . The combined organic extracts were washed with a 5% aqueous NaOH solution. The solvent was dried to yield the crude product. Products were further purified either by recrystallization or column chromatography.

**2,5-Bis(4-methoxybenzoyl)-*p*-xylene (5a).**<sup>8</sup> Washing with methanol, followed by recrystallization from ethanol afforded the cream colored product in 63% yield (mp 181–182 °C).  $^1H$  NMR (200 MHz,  $CDCl_3$ ):  $\delta$  2.24 (s, 6H), 3.88 (s, 6H), 6.92 (d,  $J$  = 8 Hz, 4H), 7.16 (s, 2H), 7.79 (d,  $J$  = 8 Hz, 2H).

**2,5-Bis(4-methoxybenzoyl)-*o*-xylene (6a).** Washing with methanol, followed by recrystallization from ethanol afforded cream colored product in 70% yield.  $^1H$  NMR (200 MHz,  $CDCl_3$ ):  $\delta$  2.18 (s, 6H), 3.86 (s, 6H), 6.90 (d,  $J$  = 8 Hz, 4H), 7.14 (s, 2H), 7.78 (d,  $J$  = 8 Hz, 4H).

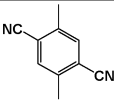
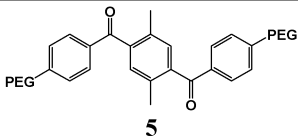
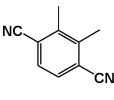
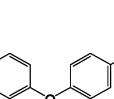
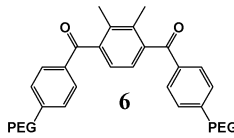
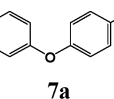
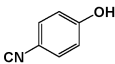
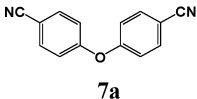
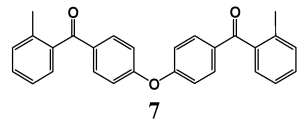
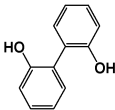
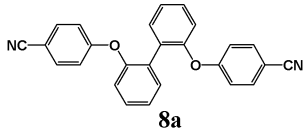
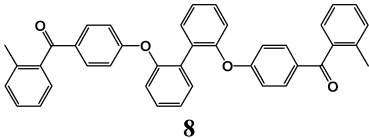
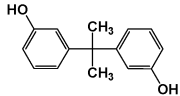
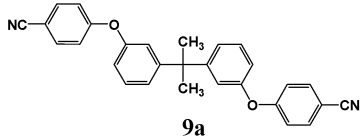
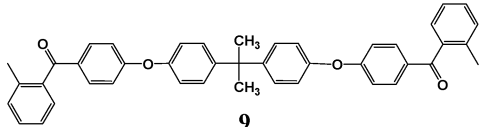
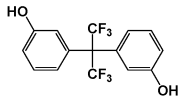
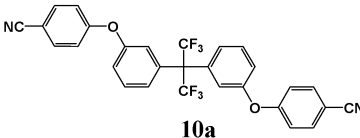
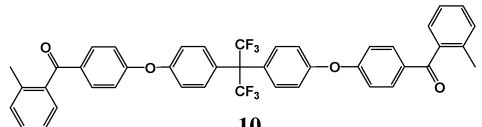
**4,4'-Bis(2-methylbenzoyl) Diphenyl Ether (7).** Column chromatography (12:1 gradient to 5:1 hexane:ethyl acetate) gave the product in 40% yield as a white solid (mp 80–81 °C).  $^1H$  NMR (200 MHz,  $CDCl_3$ ):  $\delta$  2.32 (s, 6H), 7.05 (d,  $J$  = 8 Hz, 4H), 7.23–7.38 (m, 8H), 7.81 (d,  $J$  = 8 Hz, 4H).  $^{13}C$  NMR (200 MHz,  $CDCl_3$ ):  $\delta$  197.43, 160.51, 138.78, 136.84, 133.78, 132.86, 131.31, 130.51, 128.51, 125.51, 119.00, 20.20. Mass ( $m/z$ ): 406.5, calcd; 407.2, found. IR (KBr,  $cm^{-1}$ ): 3094.0, 3064.4, 3010.0, 2954.0, 2922.5, 2860.0, 1655.2, 1584.2, 1499.7, 1485.6, 1452.8, 1421.0, 1310.6, 1293.8, 1251.0, 1171.3, 1149.5, 1109.4. Anal. Calcd for  $C_{28}H_{22}O_3$ : C, 82.64; H, 5.46. Found: C, 82.50; H, 5.45.

**2,2'-Bis(4-(2-methylbenzoyl)phenoxy)biphenyl (8).** Column chromatography (6:1 hexane:ethyl acetate) gave a white solid in 81% yield (mp 58–60 °C).  $^1H$  NMR (300 MHz,  $CDCl_3$ ):  $\delta$  2.29 (s, 6H), 6.82 (d,  $J$  = 10 Hz, 4H), 7.01 (d,  $J$  = 10 Hz, 2H), 7.20–7.42 (m, 14H), 7.66 (d,  $J$  = 10 Hz, 4H).  $^{13}C$  NMR (300 MHz,  $CDCl_3$ ):  $\delta$  197.17, 161.91, 152.99, 138.91, 136.34, 132.19, 132.07, 130.92, 130.05, 129.99, 129.34, 128.07, 125.22, 124.56, 120.12, 117.28, 19.84. Mass ( $m/z$ ): 574.7, calcd; 575.4, found. IR (KBr,  $cm^{-1}$ ): 3060.7, 3021.2, 2925.2, 1659.6, 1599.0, 1577.9, 1499.3, 1473.7, 1427.2, 1306.4, 1292.1, 1254.3, 1240.0, 1198.0, 1169.0, 1149.1, 1110.8. Anal. Calcd for  $C_{40}H_{30}O_4$ : C, 83.60; H, 5.26. Found: C, 83.37; H, 5.28.

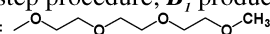
**2,2-Bis(2-(4-(2-methylbenzoyl)phenoxy)phenyl)propane (9).** Column chromatography (6:1 to 4.5:1 hexane:ethyl acetate) gave a white solid in 44% yield (mp 56–59 °C).  $^1H$  NMR (300 MHz,  $CDCl_3$ ):  $\delta$  1.74 (s, 6H), 2.34 (s, 6H), 7.02 (d,  $J$  = 10 Hz, 8H), 7.26–7.42 (m, 12H), 7.95 (d,  $J$  = 10 Hz, 4H).  $^{13}C$  NMR (300 MHz,  $CDCl_3$ ):  $\delta$  197.19, 162.25, 153.63, 146.89, 138.95, 136.31, 132.43, 132.51, 130.89, 129.95, 128.34, 128.03, 125.17, 119.72, 117.11, 42.39, 30.99, 19.80. Mass ( $m/z$ ): 616.7, calcd; 617.3, found. IR (KBr,  $cm^{-1}$ ): 3059.0, 3037.6, 2966.5, 2927.3, 2871.4, 1659.8, 1591.2, 1597.7, 1451.5, 1405.6, 1383.6, 1363.6, 1307.1, 1291.5, 1269.4, 1240.0, 1206.1, 1170.2, 1148.3, 1108.8, 1080.5, 1013.6. Anal. Calcd for  $C_{44}H_{36}O_4$ : C, 83.74; H, 5.88. Found: C, 83.44; H, 5.87.

**2,2-Bis(2-(4-(2-methylbenzoyl)phenoxy)phenyl)-1,1,1,3,3,3-hexafluoropropane (10).** Column chromatography (6:1 hexane:ethyl acetate) followed by ethanol digestion produced the target product as a white solid in 24% yield (mp 148 °C).  $^1H$  NMR (200 MHz,  $CDCl_3$ ):  $\delta$  2.31 (s, 6H), 7.03 (d,  $J$  = 8 Hz, 8H), 7.22–7.42 (m, 12H), 7.79 (d,  $J$  = 8 Hz, 4H).  $^{13}C$  NMR (200 MHz,  $CDCl_3$ ):  $\delta$  197.43, 161.01, 156.66, 138.88, 138.81, 136.72, 133.35, 133.29, 132.88, 132.21, 131.22, 130.39,

Table 1. Tabulated Synthetic Methodology

Starting Material	Rx	Dinitrile	Rx <sup>a</sup>	bis( <i>o</i> -Methylphenyl Ketone) <sup>b</sup>
---	---		<b>B<sub>1</sub> (5a)</b>	
---	---		<b>C (5b)</b> <b>D</b>	<b>5</b>
---	---		<b>B<sub>1</sub> (6a)</b>	
---	---		<b>C (6b)</b> <b>D</b>	<b>6</b>
	<b>A</b>		<b>B<sub>2</sub></b>	
	<b>A</b>		<b>B<sub>2</sub></b>	
	<b>A</b>		<b>B<sub>2</sub></b>	
	<b>A</b>		<b>B<sub>2</sub></b>	

<sup>a</sup>Reaction description of **5** and **6** are shown in sequence. For example, **5** was synthesized from the appropriate dinitrile using a three step procedure; **B<sub>1</sub>** produces **5a**, **C** gives **5b**, and **D** affords the final product **5**.

<sup>b</sup>PEG = 

129.15, 128.38, 125.48, 119.28, 118.44, 20.16. Mass (*m/z*): 724.7, calcd; 725.3, found. IR (KBr, cm<sup>-1</sup>): 3070.3, 3019.3, 2970.8, 2927.6, 1656.5, 1594.4, 1510.1, 1500.0, 1455.5, 1418.1, 1380.6, 1294.6, 1245.0, 1206.1, 1173.8, 1149.6, 1135.6, 1112.8, 1018.0. Anal. Calcd for C<sub>44</sub>H<sub>30</sub>O<sub>4</sub>F<sub>6</sub>: C, 71.27; H, 4.13. Found: C, 70.25; H, 4.16.

**General Deprotection (C).** To a 250 mL round-bottom flask were added the methoxy protected diketone (10–20 mmol), 48% HBr in H<sub>2</sub>O (100 mL), and 50 mL of acetic acid. The mixture was refluxed for 18 h and then allowed to cool to room temperature. The reaction mixture was then added to 200 mL of cold water and filtered to collect the cream colored solid product.

**2,5-Bis(*p*-hydroxybenzoyl)-*p*-xylene (5b).**<sup>8</sup> Recrystallization from methanol gave the title compound as a white solid in a yield of 77% (mp 296–299 °C). <sup>1</sup>H NMR (200 MHz, *d*<sub>6</sub>-DMSO): δ 2.16 (s, 6H), 6.89 (d, *J* = 8 Hz, 4H), 7.21 (s, 2H), 7.65 (d, *J* = 8 Hz, 2H), 10.59 (broad s, 2H).

**2,5-Bis(*p*-hydroxybenzoyl)-*o*-xylene (6b).** The crude product was dissolved in hot methanol, filtered to remove insoluble impurities, and evaporated to dryness. The white compound was recovered in 91% yield (mp 258–262 °C). <sup>1</sup>H NMR (200 MHz, *d*<sub>6</sub>-DMSO): δ 2.10 (s, 6H), 6.88 (d, *J* = 8 Hz, 4H), 7.15 (s, 2H), 7.63 (d, *J* = 8 Hz, 4H), 10.58 (s, 2H).

**General Addition of PEG (D).** To a 200 mL round-bottom flask were added the deprotected diketone (1 equiv, ca. 9 mmol), K<sub>2</sub>CO<sub>3</sub> (3 equiv, ca. 27 mmol), and dimethylformamide (DMF) (30 mL). The mixture was stirred at 55 °C for 0.5 h under N<sub>2</sub>, and a solution of PEG–TOS (2 equiv, ca. 18 mmol) in 10 mL of DMF was added dropwise. The resulting mixture

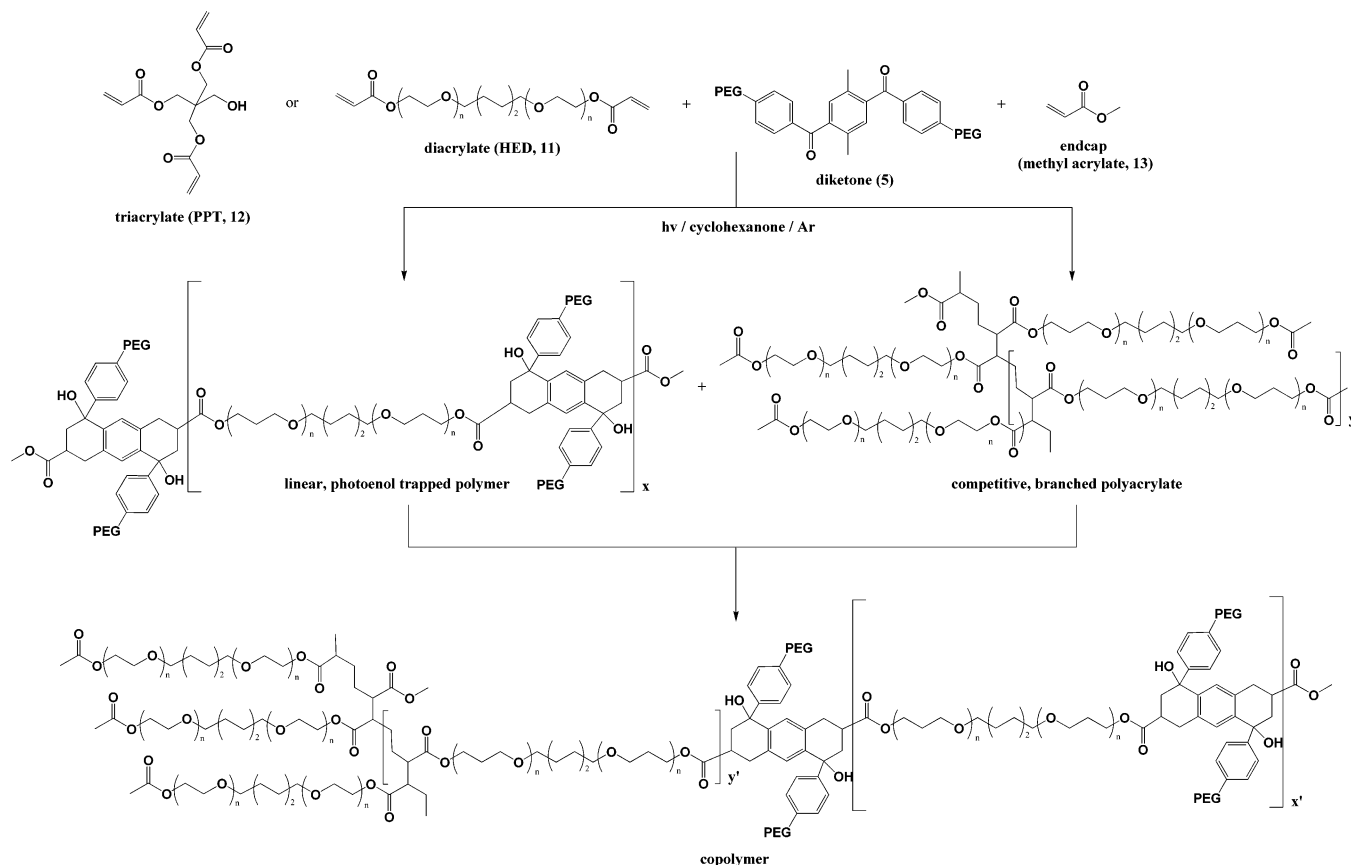
was stirred at 75 °C for 18 h and then cooled to room temperature. The solvent was evaporated in vacuo and 150 mL of diethyl ether was added to the resulting crude product. The organic extract was then washed with H<sub>2</sub>O (2 × 30 mL), 5% solution of aqueous NaOH (2 × 30 mL), and brine (2 × 30 mL) and finally dried over Na<sub>2</sub>SO<sub>4</sub>. Concentration in vacuo yielded yellow oil that solidified gradually to form the cream colored solid product.

**2,5-Bis(*p*-(tetra(ethylene glycol)oxy)benzoyl)-*p*-xylene (5).**<sup>8</sup> 86% yield (mp 54–55 °C). <sup>1</sup>H NMR (200 MHz, CDCl<sub>3</sub>): δ 2.24 (s, 6H), 3.38 (s, 6H), 3.50–3.73 (m, 16H), 3.89 (t, *J* = 2 Hz, 4H), 4.21 (t, *J* = 2 Hz, 4H), 6.94 (d, *J* = 10 Hz, 4H), 7.17 (s, 2H), 7.78 (d, *J* = 10 Hz, 4H). <sup>13</sup>C NMR (200 MHz, CDCl<sub>3</sub>): δ 196.83, 163.18, 140.61, 132.88, 132.41, 130.23, 129.80, 114.40, 71.45, 70.86, 70.62, 70.53, 69.45, 67.71, 58.94, 19.09. Mass (*m/z*): 638.7, calcd; 639.4, found. IR (KBr, cm<sup>-1</sup>): 2926.2, 2870.7, 2816.7, 1652.3, 1600.5, 1573.9, 1509.1, 1467.3, 1455.6, 1423.3, 1387.5, 1351.3, 1312.2, 1298.5, 1283.9, 1252.0, 1217.0, 1197.1, 1174.5, 1146.0, 1133.4, 1100.9, 1073.2, 1054.3, 1029.5. Anal. Calcd for C<sub>36</sub>H<sub>46</sub>O<sub>10</sub>: C, 67.92; H, 7.26. Found: C, 67.87; H, 7.24.

**2,5-Bis(*p*-(tetra(ethylene glycol)oxy)benzoyl)-*o*-xylene (6).** 86% yield (mp 49–50 °C). <sup>1</sup>H NMR (200 MHz, CDCl<sub>3</sub>): δ 2.20 (s, 6H), 3.38 (s, 6H), 3.50–3.70 (m, 16H), 3.89 (t, *J* = 2 Hz, 4H), 4.21 (t, *J* = 2 Hz, 4H), 6.96 (d, *J* = 10 Hz, 4H), 7.16 (s, 2H), 7.82 (d, *J* = 10 Hz, 4H). <sup>13</sup>C NMR (300 MHz, CDCl<sub>3</sub>): δ 197.51, 163.19, 141.06, 135.07, 132.60, 130.16, 124.21, 114.27, 71.86, 70.84, 70.56, 69.42, 67.66, 59.02, 16.91. Mass (*m/z*): 638.7, calcd; 639.4, found. IR (KBr, cm<sup>-1</sup>): 2873.7, 2822.1, 1648.4, 1599.7, 1573.6, 1508.5, 1459.3, 1421.6, 1402.8,



**Scheme 2. Schematic Representation of the Photo-Induced Polymerization of a Bis(*o*-methylphenyl ketone) (5 Shown Here) with 1,6-Hexanediol Ethoxylate Diacrylate (HED, 11) Dieneophile and Methyl Acrylate (13) End-Cap**



1399.0, 1351.4, 1311.5, 1298.9, 1252.0, 1202.3, 1166.2, 1132.3, 1102.0, 1057.0, 1031.6. Anal. Calcd for  $C_{36}H_{46}O_{10}$ : C, 67.92; H, 7.26. Found: C, 67.72; H, 7.26.

**Characterization.**  $^1H$  and  $^{13}C$  NMR spectra of the ketones were obtained on a Bruker AC 200 or Avance 300 MHz spectrometer.  $CDCl_3$  or  $d_6$ -DMSO containing TMS as an internal reference was used as the solvent for solution spectra as indicated. Solid  $^{13}C$  NMR data were acquired on a Bruker Avance 300 spectrometer using cross-polarization and magic angle spinning at a rate of 7 kHz. A TOSS routine was employed to suppress spinning sidebands. Solid spectra were externally referenced to the carbonyl of glycine which appears at 176.1 relative to TMS. Irradiation studies were performed using a Fusion UV Systems HP-6 equipped with a high-powered six-inch UV lamp system and a VPS-3 power supply. IR spectra of monomers were recorded in KBr pellets using a Nicolet 510P FTIR spectrophotometer. Mass spectral data were measured on a Finnegan LCQ (atmospheric pressure ionization) in positive ion mode with an inlet temperature of 180–220 °C. DSC experiments were run on a modulated ( $\pm 0.5$  °C/40 s) TA Instruments Q1000. The heating profile was set to 5 °C/min and run from –90 to +300 °C under nitrogen atmosphere. TGA data were collected on a TA Instruments model 1000, under nitrogen atmosphere, and with a ramp rate of 5 °C/min from room temperature to 750 °C.

**Film Preparation.** A solution of the appropriate bis(*o*-methylphenyl ketone) (5–10), 1,6-hexanediol ethoxylate diacrylate (HED, 11), Pentaerythritol triacrylate (PPT, 12) and methyl acrylate (13) in cyclohexanone were transferred into a standard aluminum weighing pan and placed in an inerting chamber. The chamber was then purged with a stream of argon for 5 min and passed under the UV irradiation source, a Fusion UV Systems HP-6. The UV lamp intensity was set at 65% and the belt speed at 2 (approximately 2 min per pass). After each pass the chamber was allowed to cool for 2 min.

The resulting materials were further dried in a vacuum oven at 55 °C for 96 h then 90 °C for 24 h.

## Results and Discussion

A series of diketones (5–10) in which two *o*-methylbenzoyl moieties are connected by linking groups of various lengths, flexibility and geometry (linear, kinked and twisted) were synthesized as shown in Table 1. The ketones were produced from precursor dinitriles in moderate to high yield using standard Grignard reactions. Diketones 5 and 6 were further functionalized with triethylene glycol monomethyl ether units for the purpose of improved solubility in cyclohexanone. All diketones were characterized by standard techniques, including  $^1H$  and  $^{13}C$  NMR, mass spectroscopy, and elemental analysis. 1,6-Hexanediol ethoxylate diacrylate (HED, 11) was used as a bis-dienophile in these studies (Scheme 2). The long alkyl chain associated with this monomer contributes to the molecular mobility in the system, compensating for the loss of entropy due to chain extension. Pentaerythritol triacrylate (PPT, 12) was used as a tris-dienophile in an attempt to produce polymers with higher glass transition temperatures by the introduction of cross-linking or branching. Methyl acrylate (13) was used in all cases as an end-cap to control polymer chain length and prevent gelation.

All polymer films prepared in this study were from monomer solutions in cyclohexanone. Cyclohexanone was chosen for its high boiling point to minimize evaporation that can affect the degree of polymerization by uncontrollably varying the concentrations of the solutions. In addition, earlier studies demonstrated that

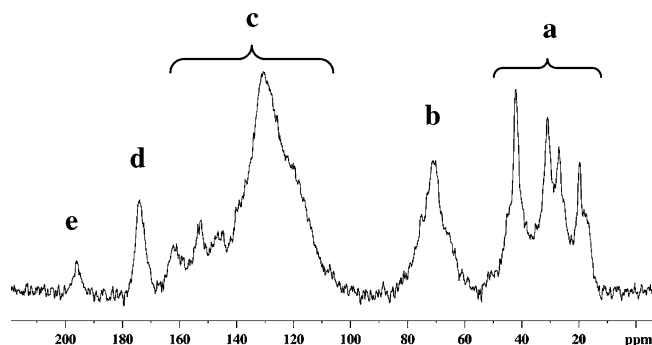


**Figure 1.** Representative  $^{13}\text{C}$  NMR spectrum for a copolymer film. The figures corresponds to the bis(*o*-methylphenyl ketone) **9** from experimental run 4.

cyclohexanone does not interfere with the desired photoenol formation step.

The temperature of the inerting chamber containing the solutions increased as it was passed under the UV lamp. In an attempt to minimize this temperature increase during polymerization, the chamber was allowed to cool under ambient conditions for 2 min between passes. It is important to note, however, that the cooling process was not suitably efficient and the temperature increased somewhat after each pass. Therefore, under our experimental conditions, thermal acrylate polymerization was a competing reaction.<sup>9</sup> This was confirmed by a control experiment in which acrylate monomer was irradiated in cyclohexanone solution under the standard experimental conditions; the monomer was observed to polymerize. Nevertheless, quantitative NMR experiments (vide infra) reveal 47–100% reaction of the bis(*o*-methylphenyl ketone)s, depending on experimental conditions and specific diketone. These data suggest the formation of copolymers with varying degrees of bis(*o*-methylphenyl ketone) incorporation.

After thorough drying, the resulting films were analyzed using various techniques. The onset of decomposition,  $T_d$ , for each film was measured in  $\text{N}_2$  by TGA analysis. Differential scanning calorimetry (DSC) was used to obtain the glass transition temperatures,  $T_g$ , for all films.

Solid  $^{13}\text{C}$  NMR spectroscopy was performed to probe the extent of reaction of the bis(*o*-methylphenyl ketone)s. Typical solid  $^{13}\text{C}$  NMR spectra of the resulting films, as shown in Figure 1, contained aliphatic peaks (a: 20–50 ppm), ethylene glycol peaks (b: 60–80 ppm), aromatic peaks (c: 110–165 ppm), and two distinct carbonyl peaks (d: 170–180 and e: 195–200 ppm). The signal at 195 ppm (e) can be assigned to unreacted diketone while the other, a broad band at 175 ppm (d), represents both unreacted and reacted acrylate. Multiple contact time experiments demonstrated that these two carbonyl peaks maintained the same ratio of peak size regardless of condition, thus allowing them to be integrated together. Initial experimental conditions were designed to include an equimolar ratio of reactive sites (i.e., one *o*-methylphenyl ketone moiety for every one acrylic ester). Since the amount of acrylate carbonyl does not change, integration of carbonyl signal intensities allows direct calculation of the percent reaction of the bis(*o*-methylphenyl ketone)s. For example, the polymer film from run 4 (diketone **9**), displays a carbonyl signal for unreacted bis(*o*-methylphenyl ketone) near 195 ppm (e) that integrates to 0.22, while the second signal near 175 ppm (d) corresponding to the acrylate carbonyls integrated to 1.00. These data may be inter-

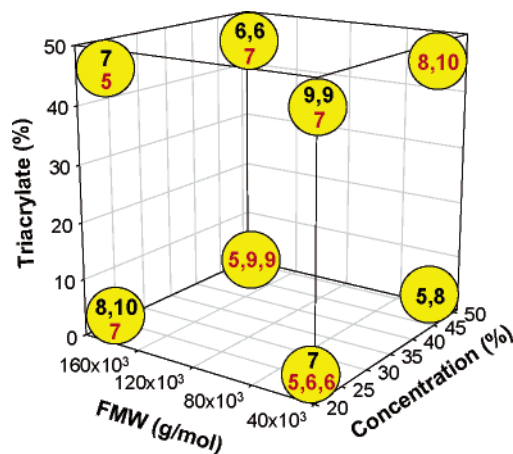


**Figure 2.** Plot of bis(*o*-methylphenyl ketone)s run in the *d*-optimal experimental design. Black displays runs at  $p = 5$  and red displays runs at  $p = 35$ .

preted as 22% unreacted bis(*o*-methylphenyl ketone), or a reaction extent of 78%.

A statistical “design of experiments” approach was used to assess the effects of photopolymerization conditions on the degree of polymerization and selected properties of the polymer films produced from each of the bis(*o*-methylphenyl ketone)s ( $k$ ) studied. Four additional variables were also chosen, including number of passes ( $p$ ) under the UV lamp, concentration of the initial solution ( $s$ ) in weight percent of monomers in cyclohexanone, end-cap mass percent ( $e$ ), and percent of triacrylate ( $t$ ) as a fraction of the total acrylates. A linear model of the following form was entertained:

$$\text{response} = A + Bp + Cs + Dt + Ek + Fe + Gps + Hpt + Ipk + Kpe + Lst + Msk + Nse + Otk + Pte + Qke$$

where  $A$  through  $Q$  are coefficients empirically derived from experimental data and response is either  $T_d$ ,  $T_g$ , or extent of reaction. The model contains terms for first-order effects of all five variables as well as all two way interaction terms for  $p$ ,  $s$ ,  $t$ ,  $k$ , and  $e$ . To evaluate linear effects of  $p$ ,  $s$ ,  $t$ , and  $e$ , a minimum of two levels of each variable must be considered. The two levels of  $p$  used were 5 and 35 passes. Solution concentration ( $s$ ) was evaluated at 20 and 51% monomer content by weight. The amount of PPT ( $t$ ) as a cross-link was evaluated at 0 and 50% of the diacrylate concentration (and concomitantly diacrylate was varied from 100 to 50%). End-cap mass percent ( $e$ ) was evaluated at 0.43 or 0.086%.<sup>10</sup> Additionally, there are six levels of the discrete variable diketone, or  $k$ , namely all of the bis(*o*-methylphenyl ketone)s (**5**–**10**).

Evaluation of the model using a full-factorial design would require 96 experiments, plus several repeats. To minimize the number of experiments in the screening study,<sup>11</sup> a *d*-optimal experimental design strategy was chosen. In this type of nonclassical design, a set of runs is computer-generated from the 96 candidate runs to evaluate the desired model most efficiently.<sup>12</sup> The scope of the design can be described using a three-dimensional box (Figure 2). The three axes of the box represent three continuous variables ( $s$ ,  $t$ , and  $e$ ). The numbers in the box represent each of the six diketones and are positioned according to the conditions of the experimental run. The remaining continuous variable ( $p$ ) is repre-

**Table 2. Experimental Design and Corresponding Data for Copolymer Films Containing 5–10**

run	diketone ( <i>k</i> )	concn % ( <i>s</i> ) <sup>a</sup>	PPT % ( <i>t</i> ) <sup>b</sup>	no. of passes ( <i>p</i> ) <sup>c</sup>	end cap (%, <i>e</i> )	<i>T</i> <sub>g</sub> (°C)	<i>T</i> <sub>d</sub> (°C)	extent of reacn (%) <sup>d</sup>
1	7	20	0	5	0.43	13.9	294	74
2	7	51	50	35	0.086	22.8	293	75
3	5	20	50	35	0.086	2.6	338	92
4	9	20	50	5	0.43	39.5	343	78
5	9	51	0	35	0.086	33.4	352	83
6	8	20	0	5	0.086	32.9	336	49
7	6	51	50	5	0.086	−23.3	331	47
8	6	20	0	35	0.43	−4.6	351	96
9	10	20	0	5	0.086	35.2	344	56
10	10	51	50	35	0.43	22.4	335	78
11	8	51	50	35	0.43	29.8	336	80
12	5	51	0	35	0.086	−19.7	341	100
13	9	51	0	35	0.086	32.2	353	85
14	9	20	50	5	0.43	36.2	340	69
15	5	51	0	5	0.43	−23.6	348	47
16	6	51	50	5	0.086	−27.3	340	53
17	8	51	0	5	0.43	30.2	327	46
18	6	20	0	35	0.43	1.2	337	88
19	7	20	0	35	0.086	35.6	323	71
20	7	20	50	5	0.086	16.2	287	78
21	7	20	50	35	0.43	33.6	314	71
22	5	20	0	35	0.43	−4.0	346	92

<sup>a</sup> Mass percent of reagents in the total mixture. <sup>b</sup> Percent of triacrylate with respect to reactive sites (i.e., two triacrylates equal three diacrylates). <sup>c</sup> Belt setting of 2 (approximately 2 min per pass) with 2 min cool between passes. <sup>d</sup> From NMR integration, see text for details.

**Table 3. Significant Terms and Summary Statistics for Models**

response	significant terms	<i>R</i> <sup>2</sup>	standard (rms) error
extent of reaction	<i>p</i> , <i>k</i> , <i>k</i> * <i>p</i> , <i>s</i> * <i>p</i>	0.982	3.48%
<i>T</i> <sub>g</sub>	<i>k</i> , <i>s</i> , <i>p</i> , <i>e</i> , <i>k</i> * <i>s</i> , <i>s</i> * <i>p</i>	0.997	2.32 °C
<i>T</i> <sub>d</sub>	<i>k</i> , <i>t</i> , <i>t</i> * <i>e</i> , <i>s</i> * <i>p</i>	0.957	5.04 °C

sented by the color scheme. The total number of unique experiments shown in the *d*-optimal design is 18. In addition, four runs from across the design were repeated to assess model reliability and accuracy, assuming error is consistent across the whole design. Table 2 shows the random order of the 22 total film-curing experiments along with the corresponding experimental data.

A mathematical model for each of the three measured responses (*T*<sub>d</sub>, *T*<sub>g</sub>, and extent of reaction) was derived using multiple linear least-squares regression.<sup>12</sup> All independent variables were transformed to the −1 to +1 range prior to modeling to minimize correlation among terms. Terms deemed not to be statistically significant (<90% confidence) were dropped from the model one at a time by the stepwise modeling technique. Linear response surfaces for each of the diketones were generated and stacked in three dimensions (response vs variable 1 vs variable 2, while holding the other two variables constant). The model terms and summary statistics are shown in Table 3. Below are selected examples of response surface models for *T*<sub>d</sub>, *T*<sub>g</sub>, and extent of reaction with related discussion.

Extent of reaction is reported as the percent diketone consumed. Significant terms in the model included first-order effects of number of passes (*p*) under the UV lamp and ketone type (*k*). Two interactive/synergistic effects of diketone with number of passes (*k*\**p*) and initial solution concentration with number of passes (*s*\**p*) were also significant. The amounts of end-cap (*e*) and triacrylate (*t*) have no effect on extent of reaction (*e* and *t*

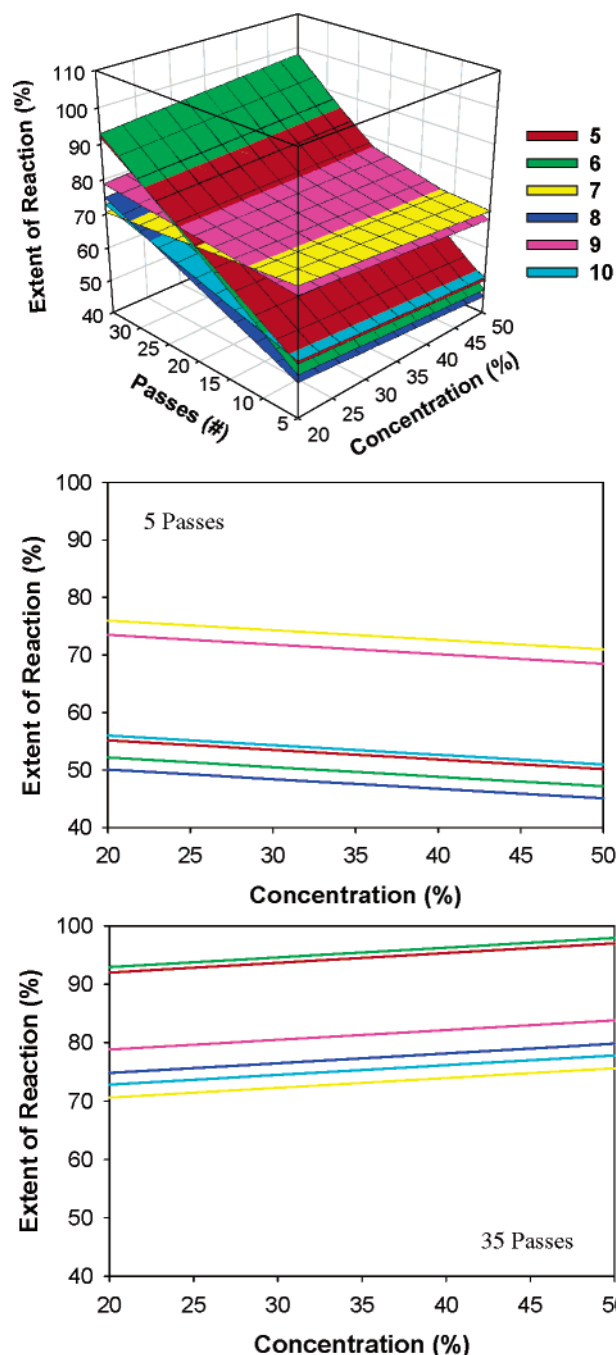


**Figure 3.** (top) Graph of the response surface model of concentration of initial solution (*s*) vs number of passes (*p*) under the UV lamp for <sup>13</sup>C NMR (extent of reaction) data. Surfaces represent fixed end-cap mass percent (*e*) of 0.086%. Percent triacrylate (*t*) was not significant and therefore could not be graphed. Two-dimensional graphs represent cross sections of the response surface model at 5 passes (middle) and 35 passes (bottom).

are not significant terms in the model). This is most likely due to the fact that the reactivity of the acrylate moiety with any one diketone is the same regardless of whether it is mono-, di-, or triacrylate. Standard error of regression for the model was 3.48% with an *r*<sup>2</sup> = 0.982.

Figure 3 (top) shows a comparison of the response surface models of the extent of reaction for all six diketones graphed vs initial concentration (*s*) and number of passes (*p*). From this figure, it is evident that increasing the number of passes dramatically increases



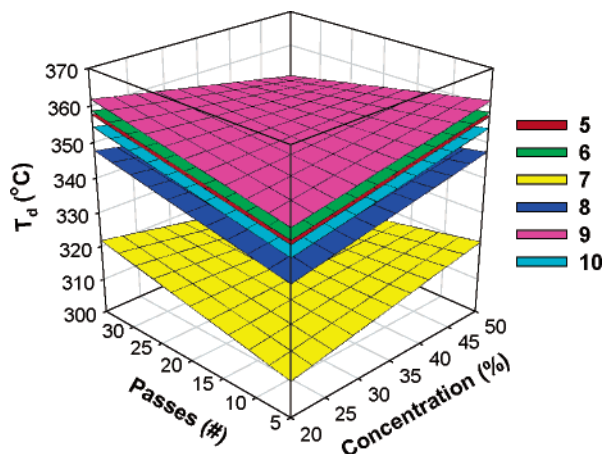


**Figure 4.** Graph of the response surface model of number of passes ( $p$ ) vs concentration of the initial solution ( $s$ ) for  $T_d$  data with fixed percent triacrylate ( $t = 0\%$ ) and end-cap mass percent ( $e = 0.086\%$ ).

the incorporation of diketone into the polymer films for **5** and **6**. There is also a moderate increase for **8** and **10**, but very little enhancement for **7** and **9**. It should be noted that number of passes directly corresponds to reaction time (i.e., amount of irradiation). During photoenol trapping, the reactive intermediate has a finite existence that requires interaction with the dieneophile before it is consumed by other reactive pathways.<sup>5</sup> Consequently, increased irradiation time enhances reaction efficiency as long as enolizable units and dieneophiles maintain their mobility and stay in solution. Thus, the major increase shown for **5** and **6** on the extent of reaction may be rationalized by enhanced solubility (and likely mobility) imparted by the PEG units. The smaller, though still statistically significant increase for extent of reaction on **8** and **10** may also be due to enhanced solubility/mobility. Insertion of a nonlinear biphenyl (**8**) as well as the use of hexafluoroisopropylidene (**10**) into otherwise linear structures are known to impart mobility in related polymers.<sup>6,13</sup>

Figure 3 (middle and bottom) also highlights the small, though statistically significant, interactive/synergistic effect between concentration and number of passes. The extent of reaction after five passes for all diketones decrease slightly with increasing concentration. After 35 passes, extent of reaction is seen to increase slightly with increasing concentration. Diels–Alder trapping of photoenols by acrylate (vide supra) is in competition with self-polymerization of the acrylates. Since the Diels–Alder cyclopolymerization process is a bimolecular reaction, increasing the concentration of both monomers will increase the effective rate constant for Diels–Alder cyclopolymerization leading to a higher extent of reaction and incorporation of the short-lived photoenols.<sup>5</sup> The rate constant for Diels–Alder trapping of *o*-methylbenzophenone derived photoenol with maleic anhydride in acetonitrile is reported to be  $2.2 \times 10^6$  M/s.<sup>14</sup>

The order of reactivity of the diketones changes from low and high passes (Figure 3 middle and bottom). At five passes, **7** and **9** show the largest extent of reaction, followed by **10** and **5**, then **6** and **8**, while at 35 passes, **5** and **6** are the most converted, followed by **9**, **8**, **10**, and then **7**. Surprisingly, **7** and **9** are at best only 85% reacted, even though after 5 passes they are already at greater than 70% conversion. It is reasonable to suggest that the photoenols generated from diketones **7** and **9**

**Table 4.** Bis-Adducts for the Photolysis and Trapping of the Bis(*o*-methylphenyl ketones) (**5**–**10**)

Ketone	Bis-Adduct <sup>a</sup>
<b>5</b> <sup>b</sup>	
<b>6</b> <sup>b</sup>	
<b>7</b>	
<b>8</b>	
<b>9</b>	
<b>10</b>	

<sup>a</sup>Bis-adducts are shown as one possible isomer.

<sup>b</sup>R =

are actually more reactive but, because the polymers come out of solution at a fairly low extent of conversion, they do not react to completion. By the same reasoning, the polymers from diketones **5** and **6** go to nearly complete conversion after 35 passes because they remain soluble.

Significant terms in the model for the onset of decomposition,  $T_d$ , include first-order effects of amount of triacrylate ( $t$ ) as the cross-linking reagent. Synergistic/interactive effects of end-cap mass percent with triacrylate concentration ( $e^*t$ ) and initial concentration with number of passes ( $s^*p$ ) were also significant. Standard error of regression for the model was 5.04 °C with an  $r^2 = 0.957$ .

A graph of the response surface for  $T_d$  vs number of passes ( $p$ ) and initial concentration ( $s$ ) is presented in Figure 4. For all diketones, the combination of five passes and low initial concentration gives films with the lowest onsets of decomposition. As the number of passes or the initial concentration is increased, the  $T_d$  of the

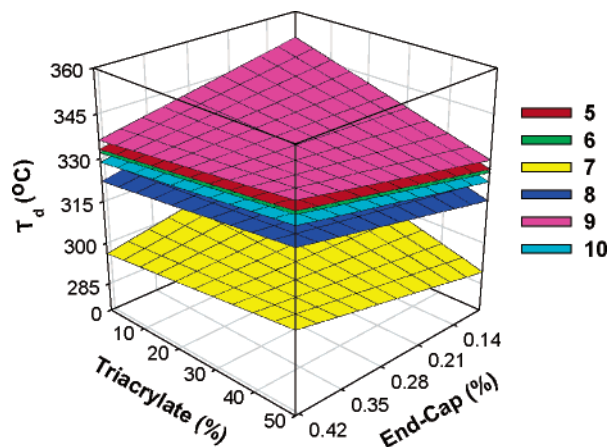


**Figure 5.** Graph of the response surface model of number of amount of triacrylate ( $t$ ) vs end-cap mass percent ( $e$ ) for  $T_d$  data. All surfaces represent a fixed initial concentration ( $s = 50\%$ ) and number of passes under the irradiation source ( $p = 35$ ). In this figure, the surface for diketone **6** is just below that for **5**.

resulting films increased. However, with a combination of high number of passes and high initial concentration, the  $T_d$  is again decreased.

Comparing Figure 4 with Figure 3 provides further insight into the reaction of the bis(*o*-methylphenyl ketone)s under the identical experimental parameters discussed above. Figure 3 shows, in general, a maximum extent of reaction of the bis(*o*-methylphenyl ketone)s for films produced with the highest initial solids concentration and 35 passes. However, the onset of decomposition (or  $T_d$ ) of these films is lower than for samples produced with either low initial concentration or low number of passes. Under the extreme condition of high initial concentration and prolonged irradiation, it is reasonable to suggest an increase of thermal acrylate polymerization, not detectable by NMR, is the reason for the shift in  $T_d$  data.

The onset of decomposition of polymer films made from the various diketones follows the order **9** > **6**  $\approx$  **5** > **10** > **8**  $\gg$  **7** based on highest to lowest onset of decomposition. Curiously, diketone **9** has the highest  $T_d$  under all conditions even though it is well above **6** and **5** in extent of reaction at five passes and falls well below **6** and **5** in extent of reaction at 35 passes. Inspection of the bis(*o*-methylphenyl ketone)s in Table 4 reveals the bis-adduct of **9** as a larger molecule with more aromatic content as compared to **6** and **5**. This structural difference likely enhances the higher short term thermal stability (and the onset of decomposition) of polymers prepared from **9** even under conditions that give a lower extent of reaction.

Figure 5 shows the effect of triacrylate concentration and amount of end-cap on onset of decomposition,  $T_d$ . For all diketones, the combination of 0% triacrylate and low end-cap concentration, gives films with the maximum  $T_d$ . Cross-link density is at a minimum at these conditions, since less end-cap would favor longer chain lengths and 0% triacrylate would result in only cross-linking due to acrylate self-polymerization.

Significant terms in the model for  $T_g$  data included first-order effects of end-cap mass percent ( $e$ ), number of passes ( $p$ ), and initial concentration ( $s$ ). Interactive/synergistic effects of the monomer solids content and number of passes ( $s \cdot p$ ) as well as the type of diketone and monomer solids content ( $k \cdot s$ ) were also significant.

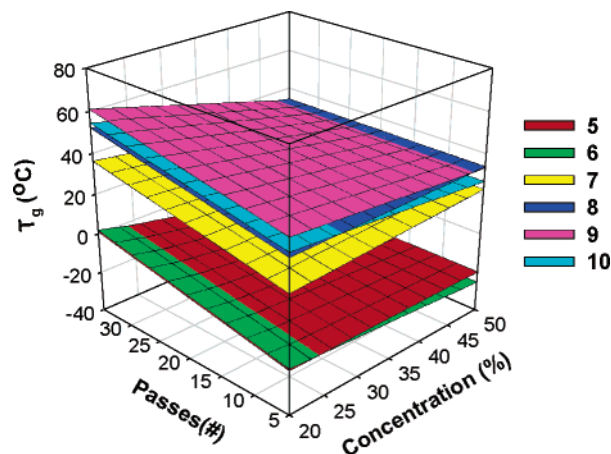


**Figure 6.** Graph of the response surface model of the number of passes ( $p$ ) vs concentration of initial solution ( $s$ ) for  $T_g$  data. Surfaces represent fixed end-cap mass percent (top:  $e = 0.086\%$ ). In this model, the amount of triacrylate is not significant.

Though triacrylate was initially included in the study as a way of increasing  $T_g$  through increased cross-linking, triacrylate concentration is not a significant term in the model. This is likely because no great increase in cross-linking is achieved by using triacrylate over and above that due to acrylate self-polymerization. Standard error of regression for the model was  $2.32^\circ\text{C}$  with an  $r^2 = 0.997$ .

A response surface model for  $T_g$  is presented in Figure 6. The PEG-functionalized bis(*o*-methylphenyl ketone)s, **5** and **6**, as expected, possess low glass transition temperatures ranging from  $-20$  to  $0^\circ\text{C}$ . The more aromatic diketones **7–10** have  $T_g$ 's ranging from  $20$  to  $60^\circ\text{C}$ . Most evident on the graph in Figure 6 is the effect of the number of passes on the  $T_g$ . Going from five to 35 passes, the  $T_g$  increases by as much as  $20^\circ\text{C}$ , in line with a higher degree of reaction of both acrylate self-polymerization and photoenol trapping. Low initial monomer concentration also resulted in increased  $T_g$  for certain diketones, probably because this condition favors photoenol trapping over acrylate self-polymerization.

## Conclusions

Irradiation of bis(*o*-methylphenyl ketone)s generates photoenols that can be trapped by acrylic esters through Diels–Alder cycloadditions. By utilizing diacrylate and triacrylate dienophiles to promote photoenol trapping, copolymer blends may be produced. This approach represents a novel process for photocured film development. A series of six new bis(*o*-methylphenyl ketone)s, **5–10**, were synthesized and evaluated for production of copolymer film. Physical properties of the resulting materials were altered by varying the photoreactive diketones and photocuring conditions. A statistically derived screening study was carried out to examine the effects of photocuring conditions for all six diketones on glass transition temperature, decomposition temperature, and extent of reaction. The resulting empirical models provided significant insight into the relationship between the reaction variables. In general, films derived from diketones with either attached PEG groups (**5** and **6**) or linking groups which impart extra molecular mobility (**8** and **10**), had a higher extent of reaction with increased time, presumably because of better solubility. Further studies will concentrate on refining the conditions for trapping the photoenols for these diketones.



In addition, continuing efforts are underway to eliminate the competing acrylate polymerization.

**Acknowledgment.** F.I. and D.S.T. are supported by NASA cooperative agreements (NCC3-887 and NCC3-1089, respectively). D.D.S. was funded by the NASA Undergraduate Researcher's Program. This work was sponsored by the Alternative Energy Foundation Technologies Subproject of the Low Emission Alternative Power Project and the Internal Research and Development Fund at the NASA Glenn Research Center.

## References and Notes

- (1) (a) Stenzenberger, H. D. In *Polyimides and Other High-Temperature Polymers*; Abadie, M. J., Sillion, B., Eds.; Elsevier: New York, 1991. (b) Itoh, T. *Prog. Polym. Sci.* **2001**, *26*, 1019–1059.
- (2) (a) Tan, L.-S.; Arnold, F. E.; Soloski, E. J. *J. Polym. Mater. Sci., Polym. Chem. Ed.* **1988**, *26*, 3103–17. (b) Hahn, S. F.; Martin, S. J.; McKelvy, L. M. *Macromolecules* **1993**, *26*, 3870–3877.
- (3) (a) Meador, M. A. *NASA TM 89836*, **1987**. (b) Meador, M. A. B.; Williams, L. L.; Scheiman, D. A.; Meador, M. A. *Macromolecules*, **1996**, *29*, 8983–8986. (c) Meador, M. A.; Kinder, J. D.; Kirby, J. P.; Tyson, D. S. Manuscript in preparation.
- (4) Yang, N. C.; Rivas, C. J. *J. Am. Chem. Soc.* **1961**, *83*, 2213.
- (5) For further information concerning the reactivity of quonodimethanes see: (a) Segura, J. L.; Martin, N. *Chem. Rev.* **1999**, *99*, 3199–246. (b) Wagner, P. J.; Sobczak, M.; Park, B.-S. *J. Am. Chem. Soc.* **1998**, *120*, 2488–2489.
- (6) Meador, M. A. *Annu. Rev. Mater. Sci.* **1998**, *28*, 599–630.
- (7) Szabó, C.; Mabley, J. G.; Moeller, S. M.; Shimanovich, R.; Pacher, P.; Virág, L.; Soriano, F. G.; Van Duzer, J. H.; Williams, W.; Salzman, A. L.; Groves, J. T. *Mol. Med.* **2002**, *8* (10), 571–580.
- (8) Although previously reported, the synthesis of **5** is presented here with additional characterization. For details, see: Ilhan, F.; Tyson, D. S.; Meador, M. A. *Chem. Mater.* **2004**, *16*, 2978–2980.
- (9) (a) Billmeyer, F. W., Jr. *Textbook of Polymer Science*; Interscience Publishers: New York, 1965. (b) Ravve, A. *Principles of Polymer Chemistry*; Plenum Press: New York, 1995.
- (10) These values of end cap percent would correspond to a formulated molecular weight of 40K and 200K, respectively, if the acrylate did not self-polymerize.
- (11) Due to limited quantities of the bis(*o*-methylphenyl ketone)s and the fundamental nature (i.e. proof-of-concept approach) of the experimental design, our objective was to minimize the number of runs while maintaining statistical significance.
- (12) *Rs/1 and RS/Discover*; Domain Manufacturing, Inc.: Burlington, MA, 1999.
- (13) (a) Liou, G.-S.; Murayama, M.; Kakimoto, M.-A.; Imai, Y. *Polym. Sci. Polym. Chem. Ed.* **1993**, *31*, 2499–506. (b) Eashoo, M.; Sen, D.; Wu Z.; Lee, C. L.; Harris, F. W.; Cheng, S. Z. D. *Polymer* **1993**, *34*, 3209–15. (c) Cheng, S. Z. D.; Wu, Z.; Eashoo, M.; Hsu, S. L.-C.; Harris, F. W. *Polymer* **1991**, *32*, 1803–10. (d) Rodger, H. G.; Guadiana, R. A.; Hollised, W. C.; Kalyanaraman, P. S.; Manello, J. S.; McGowan, C.; Minns, R. A.; Sahatjian, R. *Macromolecules* **1985**, *18*, 1058–68.
- (14) Takahashi, Y.; Miyamoto, K.; Sakai, K.; Ikeda, H.; Miyashi, T.; Ito, T.; Tabohashi, K. *Tetrahedron Lett.* **1996**, *37*, 5547–5550.

MA048291+